mRNA deadenylation by PARN is essential for embryogenesis in higher plants

SERGEI V. REVERDATTO,[1] JAMES A. DUTKO,[1] JULIA A. CHEKANOVA,[1] DOUGLAS A. HAMILTON,[2] and DMITRY A. BELOSTOTSKY[1]

[1]Department of Biological Sciences, State University of New York at Albany, Albany, New York 12222, USA
[2]Department of Biology, Hartwick College, Oneonta, New York 13820, USA

ABSTRACT

Deadenylation of mRNA is often the first and rate-limiting step in mRNA decay. PARN, a poly(A)-specific 3′ → 5′ ribonuclease which is conserved in many eukaryotes, has been proposed to be primarily responsible for such a reaction, yet the importance of the PARN function at the whole-organism level has not been demonstrated in any species. Here, we show that mRNA deadenylation by PARN is essential for viability in higher plants (*Arabidopsis thaliana*). Yet, this essential requirement for the PARN function is not universal across the phylogenetic spectrum, because PARN is dispensable in Fungi (*Schizosaccharomyces pombe*), and can be at least severely downregulated without any obvious consequences in Metazoa (*Caenorhabditis elegans*). Development of the *Arabidopsis* embryos lacking PARN (AtPARN), as well as of those expressing an enzymatically inactive protein, was markedly retarded, and ultimately culminated in an arrest at the bent-cotyledon stage. Importantly, only some, rather than all, embryo-specific transcripts were hyperadenylated in the mutant embryos, suggesting that preferential deadenylation of a specific select subset of mRNAs, rather than a general deadenylation of the whole mRNA population, by AtPARN is indispensable for embryogenesis in *Arabidopsis*. These findings indicate a unique, nonredundant role of AtPARN among the multiple plant deadenylases.

Keywords: mRNA turnover, deadenylation

INTRODUCTION

The process of messenger RNA degradation is a principal component of the network of gene expression events that determine the ultimate steady-state concentration of every transcript in the cell under a myriad of conditions. Degradation of mRNA occurs through a defined sequence of steps, that is, along specific pathways. Studies in Fungi and Metazoa have led to a definition of the four major mRNA degradation pathways: (1) deadenylation-dependent decapping followed by 5′ → 3′ decay (for review, see Mitchell and Tollervey 2000; Tucker and Parker 2000; Butler 2002); (2) deadenylation-dependent 3′ → 5′ decay (Mitchell and Tollervey 2000; Tucker and Parker 2000; Butler 2002); (3) nonsense-mediated decay (NMD), that specifically targets mRNAs with premature termination codons (Chen and Shyu 2003; Lejeune et al. 2003; Mitchell and Tollervey 2003), and (4) nonstop decay, that specifically targets mRNAs lacking termination codon (Frischmeyer et al. 2002; van Hoof et al. 2002). Pathways (1), (2), and (4) are initiated by poly(A) tail shortening and/or its complete removal, collectively termed deadenylation, which often serves as a rate-determining step of the whole process. Furthermore, at least some cases of NMD also proceed via deadenylation as well (Chen and Shyu 2003; Lejeune et al. 2003; Mitchell and Tollervey 2003). Moreover, computational modeling of mRNA decay in yeast suggests that modulation of the rate of deadenylation is a very powerful way to manipulate the overall mRNA steady-state level (Cao and Parker 2001).

Deadenylation is also subject to regulation. The rate of mRNA deadenylation can be modulated by specific, portable sequence elements that are found in the mRNA 3′-UTR. For instance, AU-rich elements (AREs), such as the ones found in the 3′-UTRs of mammalian *c-fos* and GM-CSF, can confer rapid deadenylation kinetics upon the reporter mRNAs (Chen et al. 1995). Such elements appear to act as binding sites for the specific *trans*-acting factors. Re-

Reprint requests to: Dmitry A. Belostotsky, Department of Biological Sciences, State University of New York at Albany, Albany, NY 12222, USA; e-mail: dab@albany.edu; fax (518) 442-4368.

Abbreviations: PARN, poly(A)-specific 3′ → 5′ ribonuclease; PABP, poly(A) binding protein; NMD, nonsense-mediated decay; LM-PAT assay, ligation mediated poly(A) tail length assay; ARE, AU-rich element.

Article published online ahead of print. Article and publication date are at http://www.rnajournal.org/cgi/doi/10.1261/rna.7540204.

cruitment of such factors could influence deadenylation via direct recruitment of deadenylases and/or stimulation of their activity, by altering the mRNA secondary structure, by resulting displacement from mRNA, or remodeling on mRNA, of the protecting RNA binding protein(s), for example, PABP, or by targeting PABP for degradation. Moreover, such *trans*-acting factors are the likely mediators of the regulation of the mRNA deadenylation rates by extracellular stimuli, acting through signal transduction pathways (Winzen et al. 1999; Vasudevan and Peltz 2001).

Poly(A) ribonuclease (PARN) is an evolutionarily conserved factor that has been implicated in mRNA deadenylation in metazoans (Wilusz et al. 2001). PARN belongs to the RNase D family of nucleases, which is characterized by the presence of the four conserved acidic amino acid residues in the active site that coordinate divalent metal ions for catalysis. Overall, the active site of PARN functionally and structurally resembles the active site of the 3′-exonuclease domain of *Escherichia coli* DNA polymerase I (Beese and Steitz 1991; Ren et al. 2002). Metazoan PARN specifically degrades only the poly(A) tail, but not the body, of the model polyadenylated mRNA substrates in vitro, and its activity and processivity are stimulated by the mRNA 5′ m^7GpppG cap, likely via an allosteric mechanism (Dehlin et al. 2000; Gao et al. 2000; Martinez et al. 2001). *Xenopus* PARN has been shown to deadenylate those maternal transcripts that lack cytoplasmic polyadenylation element (CPE), during oocyte meiotic maturation (Copeland and Wormington 2001), and mammalian PARN has been functionally implicated in accelerated decay conferred by AREs (Lai et al. 2003), as well as in NMD (Lejeune et al. 2003).

The occurrence of mRNA deadenylation during mRNA decay in higher plants has been mostly inferred, rather than directly demonstrated. It has been proposed, based on the examination of mRNA decay products, that ~25% of the oat phytochrome A mRNA pool degrades via a deadenylation-dependent $3' \rightarrow 5'$ pathway (Higgs and Colbert 1994). Poly(A) tail length of the rice α-amylase mRNA, αAmy3, is regulated during development (Lue and Lee 1994). In a related study, αAmy3 3′-UTR has been shown to be responsible for destabilizing the αAmy3 transcript in high-sucrose media, possibly by promoting rapid deadenylation (Chan and Yu 1998). In the one of the best studied instances of the regulated mRNA deadenylation during plant development, some mRNAs in pollinated tobacco pistils were found to undergo a poly(A) tail shortening dependent on the plant hormone ethylene acting through a signal transduction cascade that involves phosphorylation and dephosphorylation events (Wang et al. 1996). Interestingly, poly(A) shortening in this system subsequently may or may not lead to the degradation of the body of the mRNA, depending on the transcript (Wang et al. 1996).

Here, we used reverse genetics to address the functional significance of the one of the potential *Arabidopsis* deadenylases, AtPARN, and to show that its function as deadenylase is essential for plant embryogenesis. Importantly, we found that only some, but not all, embryo-specific transcripts become hyperadenylated in the mutant embryos, suggesting that deadenylation of a select subset of mRNAs by AtPARN, rather than nonspecific deadenylation of the whole mRNA population, is essential for embryonic development. Furthermore, we found that PARN function is completely dispensable in *Schizosaccharomyces pombe*, and can be at least severely knocked down in *Caenorhabditis elegans* without any obvious phenotype. Thus, the essential requirement for the PARN function is not universal in eukaryotes, and could be unique to plants.

RESULTS

AtPARN is a predominantly cytoplasmic deadenylase

Two *Arabidopsis thaliana* genes, At1g55870 (hereafter called *AtPARN*) and At3g25430, encode proteins with high sequence similarity to metazoan PARN (BLAST E values of $6.5 \times e^{-39}$ and $9.8 \times e^{-21}$, respectively, upon using human PARN as a query, with sequence homology extending through at least N-terminal two-thirds of the amino acid sequence, Fig. 1). Both genes are expressed. However, whereas the *AtPARN* open reading frame (ORF) contains all of the four highly conserved acidic residues shown earlier to be essential for catalysis in the RNase D family nucleases, including human PARN (Ren et al. 2002), the At3g25430 ORF has nonconservative replacements in three of the four positions (Fig. 1). Thus, only the former is likely to encode a catalytically active PARN enzyme. This view is corroborated by the results of site-directed mutagenesis experiments on AtPARN described below, as well as the fact that the knockout of the At3g25430 gene causes no apparent phenotype (see Materials and Methods), in contrast to the embryonic lethal phenotype that is caused by the knockout of *AtPARN* (below). Purified recombinant AtPARN degraded only the poly(A) tail, not the body, of the model polyadenylated RNA substrate in vitro, and it did not degrade an otherwise identical polyuridylated substrate (Fig. 2A). Thus, AtPARN encodes a functional deadenylase enzyme.

RT-PCR based survey revealed that the *AtPARN* mRNA is broadly expressed in roots, stems, leaves, and flowers (data not shown). To address the subcellular distribution of the AtPARN polypeptide, we generated transgenic *Arabidopsis* plants bearing a genomic *AtPARN* construct containing the green fluorescent protein (GFP) ORF fused to the last exon of the *AtPARN* gene. The resulting AtPARN-GFP C-terminal fusion protein was functional, as it fully rescued the mutant phenotype of the *atparn-1* null allele (below). In the second approach, the GFP-AtPARN fusion construct driven by a strong, constitutive 35S promoter was introduced into onion epidermal cells using biolistic protocol. In both experiments, a predominantly cytoplasmic signal was

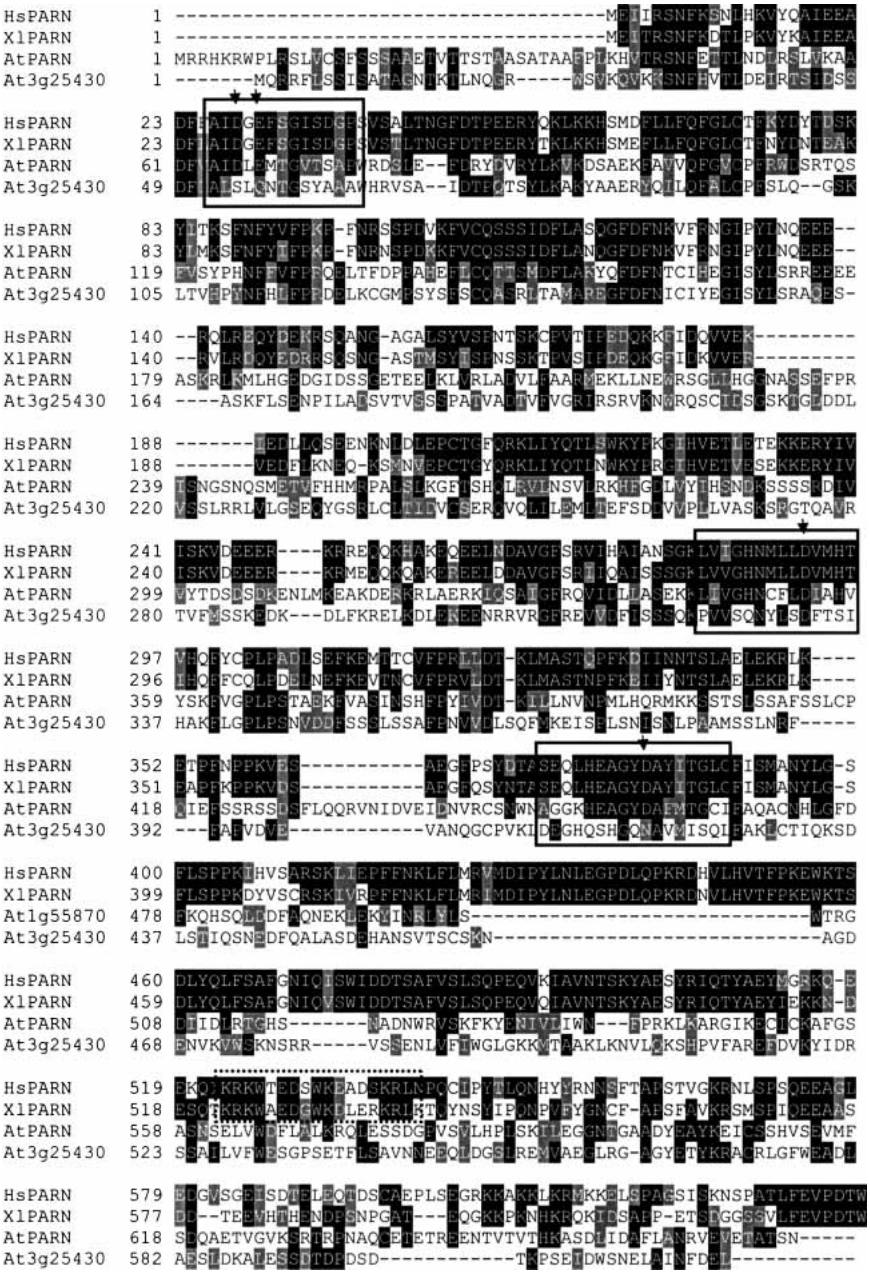

FIGURE 1. Sequence alignment of the amino acid sequences of human PARN, *Xenopus* PARN, AtPARN, and the *Arabidopsis* protein encoded by ORF At3g25430. Alignment was generated by ClustalW. The conserved ExoI, ExoII, and ExoIII domains are shown boxed. The bipartite NLS motif in human and *Xenopus* proteins is shown by dotted box. Black and gray shading designates residues that are identical or similar, respectively, in at least half of the sequences. The four acidic residues that coordinate the Mg^{++} ion for catalysis are marked by arrowheads. To produce D66A E68A mutant of AtPARN, D and E residues in the ExoI domain were replaced by alanines via site-directed mutagenesis.

observed (Fig. 2C,D). In contrast, human PARN exhibits both nuclear and cytoplasmic localization (Korner et al. 1998). In *Xenopus* oocytes, PARN is present in two isoforms, the nuclear 74-kDa and the cytoplasmic 62-kDa species, the latter probably derived by proteolytic cleavage from the 74-kDa polypeptide (Copeland and Wormington 2001). Both human and *Xenopus* PARN feature bipartite NLS in the C-terminal portion of the protein (Fig. 1). On the other hand, AtPARN lacks any obvious NLS motifs, which is consistent with its predominantly cytoplasmic localization.

Exoribonuclease activity of AtPARN is essential for plant embryogenesis

To investigate the significance of the AtPARN function for plant growth and development, several T-DNA insertional alleles of the *AtPARN* gene were isolated, and two of them (*atparn-1* and *atparn-2*, Fig. 3A) were characterized in detail. No homozygous mutant plants were recovered among the selfed progeny of plants heterozygous for either allele. Moreover, no viable transheterozygotes could be obtained by crossing the *atparn-1*/+ and *atparn-2*/+ plants, suggesting that the disruption of the *AtPARN* gene causes either zygotic or gametophytic lethality. However, reciprocal crosses have shown that the transmission of the mutant alleles through both male and female gametes was normal (data not shown), thus ruling out gametophytic lethality. On the other hand, one-quarter of the seeds obtained by selfing of the heterozygous *AtPARN*/*atparn* plants failed to accumulate chlorophyll and appeared white, in contrast to the normal seeds that underwent greening starting from the heart stage of embryo development (Fig. 3B). This is a classical hallmark of the embryonic lethal phenotype in plants (Meinke 1994). Dissection of the embryos from the green and white seeds and PCR-based genotyping showed that the white seeds contained smaller, underdeveloped embryos, all of which were *atparn/atparn* homozygous mutant (Fig. 3C). We noted that a previously described embryonic lethal mutation *emb25* maps very closely to the *AtPARN* gene (Meinke 1994); however, formal allelism tests showed that *AtPARN* and *EMB25* are distinct genes (see Materials and Methods). Thus, *Arabidopsis* PARN is a novel factor that is essential for embryogenesis.

The embryo-lethal *atparn-1* phenotype was fully rescued by the transformation with the *AtPARN* genomic fragment containing 0.9 kb of upstream flanking sequence. To dis-

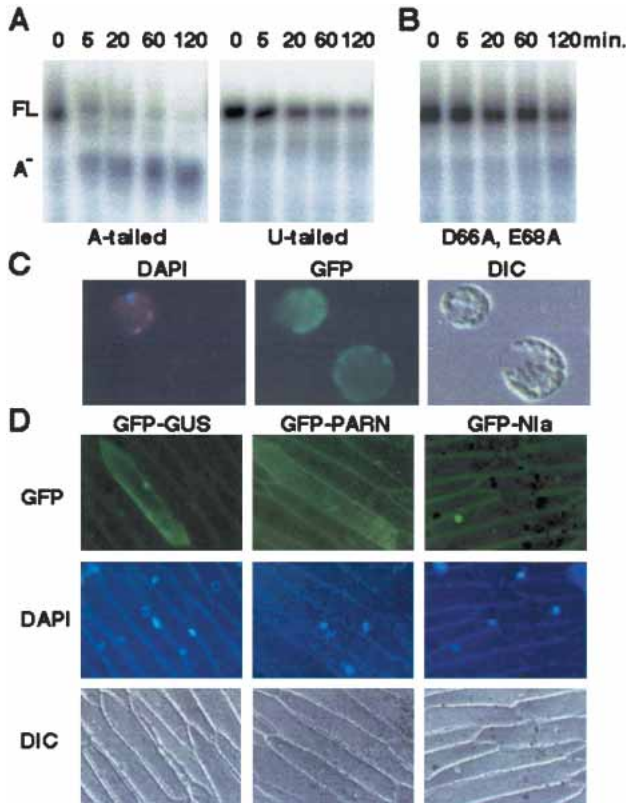

FIGURE 2. AtPARN is a predominantly cytoplasmic poly(A) exoribonuclease of an RNase D type. (*A*) Results of an in vitro assay using polyadenylated and polyuridilated synthetic RNAs of otherwise identical sequence, with wild-type recombinant AtPARN. (*B*) Results of an in vitro assay using polyadenylated RNA with the recombinant D66A E68A mutant AtPARN protein. (*C*,*D*) Localization of the AtPARN-GFP in transgenic *Arabidopsis* (*C*: protoplasts were prepared from the *atparn Arabidopsis* plants rescued by the AtPARN-GFP fusion; blue is DAPI staining for nuclei, red is chlorophyll autofluorescence of the chloroplasts) and of the GFP-AtPARN in onion epidermal cells using a biolistic assay (*D*: GFP-GUS and GFP-Nia are cytoplasmic and nuclear localized controls, respectively).

tinguish whether the lethality in the *Arabidopsis atparn* mutants occurred because of the loss of the AtPARN exoribonucleolytic activity, or of some other function associated with the AtPARN polypeptide, we substituted two of the four universally conserved acidic residues located in the ExoI domain that are essential for the activity of the RNase D type exonucleases (Ren et al. 2002) by alanines (D66A E68A mutant). Enzymatic assays of the D66A E68A mutant polypeptide that was expressed and purified from *E. coli* confirmed that these substitutions resulted in a loss of exoribonucleolytic activity (Fig. 2B). When expressed in planta, the AtPARN protein thus inactivated was unable to rescue the embryonic lethal phenotype of the *atparn* mutations, demonstrating that deadenylating activity of AtPARN is essential, at least during embryogenesis.

Microscopic examination of the selfed heterozygous plants revealed that the mutant embryos exhibited a pronounced retardation of development (Fig. 3D). *Arabidopsis* embryogenesis is characterized by a highly stereotypical progression through a series of morphologically distinguishable stages that are named according to the shape of the embryo: globular, heart, torpedo, walking-stick, and mature embryo (Bowman and Koornneef 1994). We found that by the time the normal embryos reached the heart stage of development, mutant seeds within the same siliques (seed pods) contained embryos that were still at the early globular stage; when normal embryos reached the walking-stick stage, the mutant sibling embryos were still at the late globular stage; by the time near-mature normal embryos had filled out most of the seed, mutant embryos within the same silique were still at the heart stage. We further verified that the morphology of the mutant embryos truly reflected a delayed pace of development by introducing, via crossing, the reporter gene fusions expressing β-galacturonidase (GUS) at the specific stages of embryogenesis, including FAE1::GUS (expressed from the early torpedo stage onward; Rossak et al. 2001), cotton α-globulin::GUS (expressed from the mid-torpedo stage onward; Sunilkumar et al. 2002), and 7S::GUS (expressed from the early bent cotyledon stage onward; Hirai et al. 1994; Apuya et al. 2001). For each of the three reporters, the mutant embryos were GUS-negative at the respective developmental stages, when the wild-type and heterozygous sibling embryos already exhibited robust GUS activity (Fig. 3E). The mutant embryos eventually did turn on the expression of these reporter genes (Fig. 3E, data for cotton α-globulin::GUS), but after a considerable delay. Furthermore, examination of the GFP gene trap reporter KS117, which normally expresses the green fluorescent protein throughout the endosperm during early embryogenesis but becomes restricted toward the posterior pole of the endosperm by the early globular stage (Sorensen et al. 2001), revealed that the *atparn* mutant seeds are impaired in the endosperm patterning: The posterior polarization of the KS117 expression failed to occur as late as the walking-stick stage of embryogenesis (Fig. 3F).

Mutant embryos beyond the early walking-stick stage were not observed, because at this point siliques entered desiccation. The onset of desiccation tolerance in the wild-type plants normally takes place toward the end of embryogenesis (Koornneef et al. 1989). Because of the retarded pace of development of the *atparn*/*atparn* mutant embryos, the seed desiccation in the *AtPARN*/*atparn* heterozygous plants commenced before the mutant embryos reached maturity. Thus, we reasoned that this might have explained the lethality of the *atparn* alleles. However, attempts to rescue the mutant embryos in culture did not produce any fully regenerated plants. Nevertheless, the *atparn* mutant embryos underwent multiple cell divisions, and showed cell differentiation and morphogenesis typical of normal seedling development. Many of the mutant embryos extended primary roots and produced root hairs that were correctly positioned in alternating epidermal cell files, and some of them also initiated the development of true leaves (Fig. 3G).

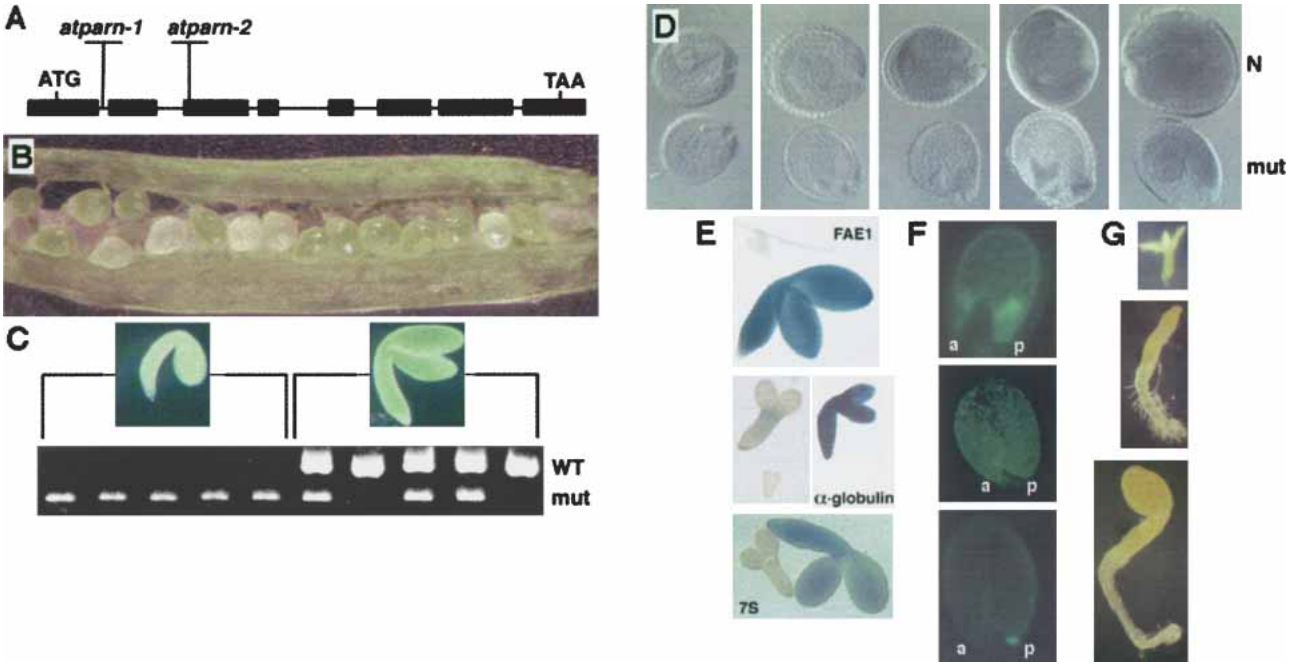

FIGURE 3. Null alleles of AtPARN lead to a slowed pace of embryogenesis and eventual arrest. (*A*) Schematic maps of the T-DNA insertion alleles *atparn-1* and *atparn-2*. (*B*) Dissected developing silique from the *atparn/AtPARN* heterozygote contains 1/4 white seeds, a classical hallmark of the embryo lethal phenotype. (*C*) PCR-based genotyping of the embryos dissected from the white and green seeds derived from the same silique. (*D*) DIC images of the developing seeds at progressively more advanced (from *left* to *right*) developmental stages; *top* row, phenotypically normal (wild-type and heterozygous) seeds, *bottom* row, mutant seeds. (*E*) Expression of the embryogenesis stage-specific marker genes in the mutant and phenotypically normal embryo pairs obtained from the selfed progeny seeds of the *atparn/AtPARN* heterozygous plants: FAE1::GUS (*top* panel), cotton α-globulin::GUS (*middle* two panels, *right* panel shows that the mutant embryos at near-terminal stages of development turn on the α-globulin::GUS reporter), and 7S::GUS (*bottom* panel). (*F*) Expression of the endosperm-specific GFP reporter KS117 becomes polarized toward the posterior pole (a, anterior; p, posterior) in the WT endosperm at the globular stage (*top*), but polarization fails to occur in the *atparn* seeds at a similar stage of development (*middle*, representative of 81 *atparn* mutant seeds examined). Normal siblings of the mutant seed (shown in the *middle* panel) contained mature embryos and showed distinct GFP expression in the posterior chalazal zone (*bottom*). (*G*) Incubation of the mutant embryos in an in vitro culture can lead to initiation of true leaves (*top left*), formation of the root hairs (*top right*), or both (*bottom* panel).

Therefore, quite extensive gene expression programs can occur in the complete absence of the AtPARN function.

Essential requirement for the PARN function is not universal across the phylogenetic spectrum

To assess the generality of the essential requirement for the function of the PARN deadenylase, representatives of Fungi and Metazoa were also examined. Remarkably, disruption of the gene encoding the PARN homolog in *S. pombe* had no apparent consequences on viability, growth rate, or sporulation (Fig. 4A–C). Moreover, no gross abnormalities in the total mRNA poly(A) tail length distribution were observed (Fig. 4D). This is likely due to a redundancy in mRNA deadenylation systems in *S. pombe* (see Discussion). In addition, the requirement for the PARN function in *C. elegans* was assessed by RNAi knockdown. *C. elegans* has two genes encoding PARN-like proteins, designated K10C8.1 and Y57A10A.25. Prior knockdown experiments targeting these two genes individually did not result in any apparent phenotype (Kamath et al. 2003). Therefore, we targeted these two genes simultaneously using a hybrid dsRNA, by both microinjection and feeding. In both cases, no visible phenotype in embryos, larvae, or adults was observed, whereas semiquantitative RT-PCR experiments showed that the expression level of both genes in feeding experiments was reduced by up to ~90% (data not shown). Although it cannot be ruled out that the residual amounts of these mRNAs were sufficient for full function in *C. elegans*, these data, taken together with the above finding in *S. pombe* and a complete absence of PARN homologs in *S. cerevisiae* and *D. melanogaster*, are consistent with the view that the essential requirement for the PARN function is not universal across the phylogenetic spectrum.

Loss of AtPARN affects poly(A) tail length distribution of only a select subset of embryonic transcripts

The effect of the loss of the AtPARN on mRNA deadenylation in embryos was assessed using a modified LM-PAT assay (Fig. 5A; Salles et al. 1999; Xie et al. 2003). In this assay, the total RNA pool extracted from the developing

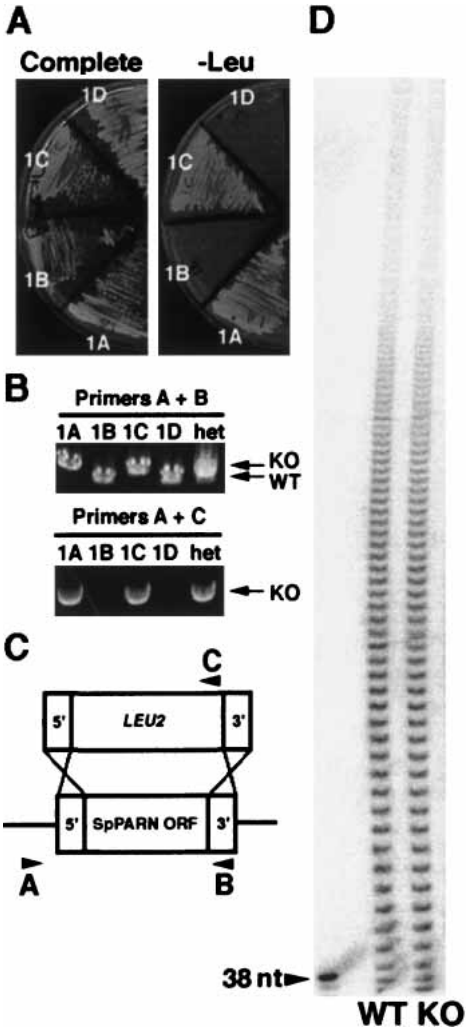

FIGURE 4. PARN function is dispensable in *S. pombe*. (*A–D*) PARN gene disruption in *S. pombe*. The *S. pombe* PARN gene was disrupted in a diploid strain as shown in *C*, and haploid meiotic progeny derived from resulting heterozygous strain were genotyped (*B*) and plated onto nonselective and selective media (*A*), as well as tested for alterations in the poly(A) tail length distribution (*D*).

wild-type or mutant seeds harvested at the torpedo stage of embryogenesis was tagged at the 3′ end via ligation of the RNA oligonucleotide whose own 3′ end was chemically blocked to prevent the formation of concatemers. The resulting tag was then used for priming the reverse transcription and for subsequent PCR using the tag-specific and the gene of interest-specific primer pair. Because the PCR amplification occurred across the poly(A) tail, the resulting PCR product length distribution was a function of the poly(A) tail length distribution of the embryonic transcript of interest. Furthermore, because the mutant seeds also contained, in addition to the zygotically derived homozygous mutant embryos, sporophytic diploid tissues that are heterozygous for the respective alleles, we examined the poly(A) tails of several transcripts selected based on the previously published information that they are expressed exclusively in embryos.

We detected no apparent differences in the poly(A) tail length distribution between mutant and wild-type embryos for cruciferin, oleosin, *LEC1*, and *LEC1*-like mRNAs. However, a significant elongation of the poly(A) tails of the *PROLIFERA* (*PRL1*) mRNA (Springer et al. 1995), which encodes the *Arabidopsis* homolog of MCM7 protein, a part of the MCM2–7 complex that functions in the initiation of DNA replication (Tye and Sawyer 2000), was observed in the mutant embryos (Fig. 5B). Importantly, no changes in the *PRL1* poly(A) tail length distribution were detected in the biotin biosynthesis-deficient *bio1-1* mutant, whose embryos arrest at a similar stage of embryogenesis. This demonstrates that the elongation of the poly(A) tails of *PRL1* mRNA is not a nonspecific consequence of an arrest of embryogenesis. It remains to be determined whether the apparent defect in the poly(A) tail shortening of the *PRL1* mRNA, which may lead to overexpression of the PRL1 polypeptide, is responsible for the defects in endosperm polarization, embryogenesis, and the eventual lethal phenotype of *atparn* mutants, but it is notable that the loss of function alleles of *PRL1* also display abnormal endosperm development and embryo lethal phenotype (Springer et al. 1995, 2000). Situations in which both overexpression and the loss-of-function alleles of a subunit of a multiprotein complex such as MCM cause similar phenotypes are not uncommon, probably because of the resulting imbalance in the concentrations of its components (Papp et al. 2003).

Most importantly, the transcript-specific differences in the effect of *atparn* null mutations on poly(A) tail length strongly indicate that AtPARN does not indiscriminately deadenylate all mRNAs in the embryos, but rather is specifically required for the poly(A) tail shortening of a select subset of embryonic transcripts. It is notable in this context that mammalian PARN was shown to be actively recruited to specific targets, such as those possessing AREs in their 3′-UTRs (Lai et al. 2003).

DISCUSSION

Mechanisms of mRNA decay in higher plants remain poorly understood. Most of the progress in this area has been made in defining and characterizing the *cis*-acting sequences that govern plant mRNA decay, such as DST (portable destabilizing element that confers constitutive instability; Gil et al. 1994; Gil and Green 1996), iLRE (light responsive element of pea *Fed-1*; Petracek et al. 1997), and possibly ARE (Ohme-Takagi et al. 1993), although no natural ARE-mediated decay substrates are known in plants, and premature termination codons (van Hoof and Green 1996; Isshiki et al. 2001). Furthermore, some plant genes have been shown and many more are suspected to be regulated at the level of mRNA of decay in response to various stimuli (e.g., ferredoxin Fed-1 by light [Petracek et al. 1997], α-amylase

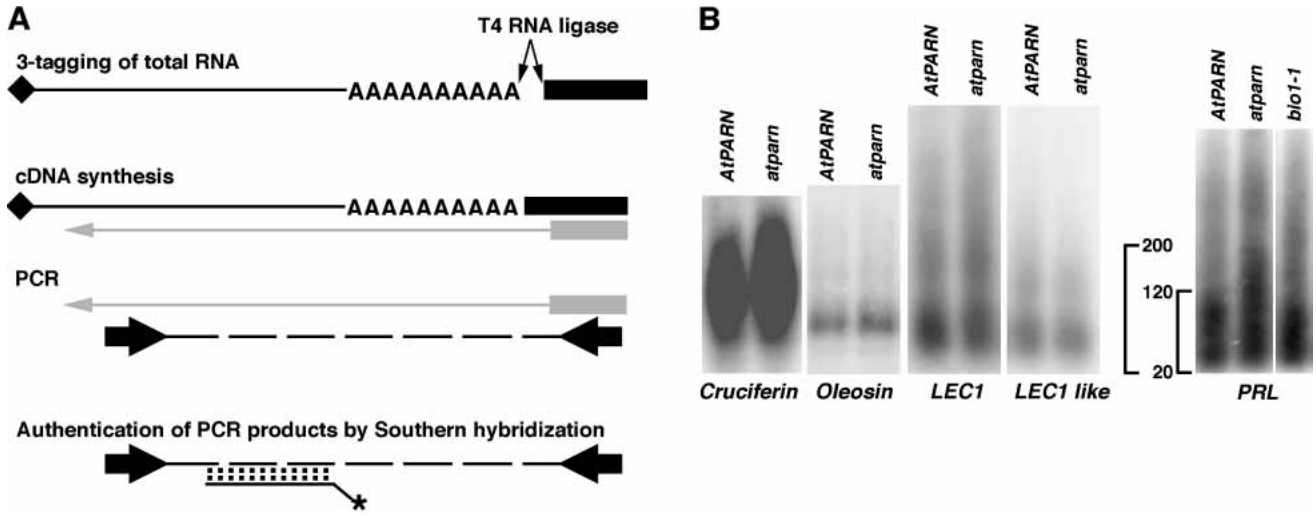

FIGURE 5. Poly(A) tail metabolism of some, but not all, embryo-specific mRNAs is impaired in the *atparn* mutant embryos. (*A*) Scheme of the LM-PAT assay used to visualize the poly(A) tail length distributions on selected embryo-specific transcripts. (*B*) LM-PAT assay results for cruciferin, oleosin, LEC1, *LEC1*-like, and PROLIFERA (*PRL*) mRNAs from *AtPARN*, *atparn*, and *bio1-1* seeds. Authenticity of the LM-PAT products in each panel was verified by hybridization with a gene-specific oligonucleotide probe. In the case of *PRL*, the validity of the length distribution of the hybridization products as a measure of the PRL mRNA poly(A) tail length distribution was additionally verified by carrying out an RNaseH/oligo(dT) cleavage prior to LM-PAT. In this case, the signal collapsed into a single band corresponding to a major polyadenylation site in PRL transcript (data not shown).

αAmy3 by carbon source [Sheu et al. 1996], and cystationine γ-synthase by AdoMet [Chiba et al. 1999, 2003]). However, the pathways and governing principles of mRNA degradation in plants remain largely obscure, with the partial exception of the degradation pathway of oat phytochrome (*PHYA*) mRNA, that seems to undergo decay in both $5' \rightarrow 3'$ and $3' \rightarrow 5'$ directions (Higgs and Colbert 1994), and of soybean *SRS4* mRNA encoding the ribulose-1, 5-bisphosphate carboxylase/oxygenase (Rubisco) small subunit, whose degradation is initiated by endonucleolytic cleavages (Tanzer and Meagher 1995). The latter is an extremely abundant message, and thus its degradation pathway may be unusual. The AdoMet-regulated, translation-dependent decay of the cystationine γ-synthase (CGS) mRNA may also be associated with endonucleolytic transcript cleavage. Yet, it is unclear how common this is, because even in case of CGS, this mechanism may not apply to other plants (Kreft et al. 2003). Yet another instance of the endonucleolytic cleavage occurs during microRNA-guided mRNA cleavage events (Llave et al. 2002; Palatnik et al. 2003; Xie et al. 2003). The latter pathway, which is related to the RNAi phenomenon in animals and posttranscriptional gene silencing (PTGS) in plants, apparently governs some key developmental decisions in plants (e.g., Chen et al. 2002; Boutet et al. 2003; Palatnik et al. 2003; Kidner and Martienssen 2004), but is unlikely to play a significant role in the general plant mRNA decay. Finally, nonsense-mediated decay (NMD) has been studied in *Arabidopsis* (van Hoof and Green 1996) and rice (Isshiki et al. 2001); however the sequence of steps, the factors involved, and the directionality of decay in both species remain unknown.

Identification of the plant mRNA decay enzymes using forward genetics in *Arabidopsis* has been attempted but has proven extremely difficult because such mutants are very rare (Johnson et al. 2000). On the other hand, in silico approaches allow investigators to tentatively identify potential homologs of many mRNA decay enzymes, including decapping enzymes (DCP1 and DCP2), 5′–3′ exonucleases (e.g., XRN1-like; Kastenmayer and Green 2000), exosome components (Chekanova et al. 2000, 2002), and multiple deadenylases that belong to several distinct classes (e.g., Dupressoir et al. 2001). Among the latter group, PARN is an evolutionarily conserved factor that has been implicated in mRNA deadenylation in metazoans (Wilusz et al. 2001). *Xenopus* PARN was shown to deadenylate those maternal mRNAs that lack cytoplasmic polyadenylation element (CPE) during oocyte meiotic maturation (Dehlin et al. 2000; Copeland and Wormington 2001), and mammalian PARN has been shown to act during NMD (Lejeune et al. 2003) and in ARE-mediated mRNA decay (Lai et al. 2003) in cultured mammalian cells. However, the significance of the PARN function at the whole-organism level has not been elucidated, and the division of labor, if any, between PARN and other deadenylation enzymes has not been addressed.

We have characterized the *Arabidopsis* PARN (AtPARN) and studied the consequences of the loss of the AtPARN function for plant viability. Results of the activity assays in vitro, coupled with the site-directed mutagenesis experiments, demonstrate that AtPARN is a poly(A)-specific exoribonuclease that belongs to the RNase D family. AtPARN appears to be localized predominantly in the cytoplasm, consistent with its role in mRNA turnover. We found that

deadenylation by PARN is essential for plant viability. The development of the *Arabidopsis* embryos lacking AtPARN, or expressing an enzymatically inactive protein, was markedly retarded, culminating in an arrest at the bent-cotyledon stage, although the *atparn* mutant embryos were capable of limited cell division, development, and differentiation in culture, indicative of the existence of AtPARN-independent gene expression programs. While the present report was in review, Chiba et al. (2004) also reported that the T-DNA insertional mutations in the *AtPARN* gene cause a lethal phenotype; however, those authors concluded that this could be due to either embryonic or gametophytic (i.e., haploid-phase) lethality. Importantly, however, neither formal analyses of male and female transmission by reciprocal crosses nor complementation experiments were conducted by those authors. In contrast, our phenotypic and genetic analyses, and in particular reciprocal crosses, rule out gametophytic lethality. We also extend our analyses to show that although AtPARN enzymatic activity is essential in a higher plant, it is dispensable in the representative of Fungi (*S. pombe*), and can be at least severely downregulated in a metazoan (*C. elegans*) without any obvious phenotype. Importantly, only some, but not all, embryo-specific transcripts examined were hyperadenylated in the mutant embryos, suggesting that deadenylation of a select subset of mRNAs, rather than of the whole mRNA population, is indispensable for embryogenesis in *Arabidopsis*. It is important to note in this regard that deadenylation of the ARE-containing mRNA substrates by mammalian PARN can be specifically stimulated by ARE-binding factors such as tristetraprolin (TTP), as was demonstrated by experiments in vitro and by cotransfection studies in human HEK293 cells (Lai et al. 2003). This stimulatory effect was dependent both on the *cis*-acting element (the ARE), and on the ability of the *trans*-acting factor (TTP) to recognize it, even though the direct TTP-PARN interactions could not be demonstrated. This could be because the interaction is transient and/or requires bridging factors, or because the TTP binding to the ARE causes remodeling of the mRNP structure, that is, it makes the polyadenylated mRNA substrate more accessible to PARN, rather than activating PARN enzyme directly. Regardless of the underlying mechanism, these and our findings suggest that the substrate specificity in PARN action is an evolutionarily conserved principle.

An important aspect of our findings is that the essential requirement of the PARN function is not universal across the phylogenetic spectrum. One potential explanation as to why Fungi and Metazoa may be more tolerant to the lack of PARN than plants is redundancy. In addition to PARN, two other deadenylation systems have been characterized in yeast and humans: poly(A) nuclease (PAN) and CCR4/CAF1 complex (Tucker et al. 2001; Uchida et al. 2004). However, the genome of *A. thaliana* encodes at least one of the PAN subunits, as well as six putative homologs of *CCR4*, at least five of which are expressed, and as many as 11 *CAF1* homologs, at least seven of which are expressed. Thus, redundancy alone cannot readily explain differences in the dependence on the PARN function between species. Rather, our findings suggest that AtPARN may be essential for regulating the poly(A) tail metabolism, and therefore translation efficiency and/or stability, of a specific subset of embryonic transcripts whose encoded products are critical for normal development.

MATERIALS AND METHODS

Plant material and genetic techniques

The *atparn* mutants were outcrossed to the wild-type WS plants twice prior to analysis. The *atparn-2* allele was subsequently moved into Ler background, in order to facilitate dissection, and used for the DIC microscopy of the embryos shown in Figure 3. Plants were grown at 23°C under 16 h light and 8 h dark. To establish that *AtPARN* is nonallelic with *EMB25*, the following criteria were used. When *EMB25/emb25* and *AtPARN/atparn2* plants were crossed, no white (i.e., mutant) seeds were observed among the F1 progeny seeds. Moreover, one-quarter of the selfed F2 progeny plants produced 50% white (mutant) seeds, rather than 25% white seeds. This could only be only possible if these plants contained two distinct embryo lethal mutations closely linked in *trans*. Furthermore, selfed F2 plants did not segregate any wild-type F3 progeny. Instead, all of the F3 progeny plants examined contained 50% white seeds, reinforcing the conclusion that their F2 parent plants contained *emb25* and *atparn* mutations closely linked in *trans*. Plant transformation was done by the floral dip method as described (Clough and Bent 1998). For the embryo rescue experiments, the early heart- to early torpedo-stage embryos were liberated from the developing seeds using insulin needles, placed on Murashige-Skoog medium with 1% sucrose and 0.7% Phytagar (Gibco), and incubated in a Percival growth chamber (23°C, 16 h light and 8 h dark) for 10–14 d, and surviving plantlets were transplanted to soil. Under these conditions, none of the mutant embryos (n = 46) and 70% of the wild-type and heterozygous (17 of 24) embryos were fully regenerated and gave raise to full-grown plants.

Plasmid constructs

Expression constructs

For initial expression trials, an ~2-kb cDNA fragment of AtPARN was amplified with primers oDB605/oDB606 and cloned into pET24a (Novagene) using NdeI and XhoI sites that are in frame with the C-terminal His tag (construct pDB574). The resulting His-tagged protein product was mostly insoluble. GST-tagged PARN (pDB586) expressed in insect Sf9 cells using a baculovirus Bac-to-Bac system (Invitrogen) was more soluble, but poorly bound to glutathione resin. For the expression in *E.coli* as a fusion with N-terminal maltose-binding protein (MBP), the cDNA fragment amplified with primers oDB632/oDB633 was cloned into both cytoplasmic (pMAL-c2X) and periplasmic (pMAL-p2X) ex-

pression vectors (New England Biolabs), using XhoI and HindIII sites, resulting in pDB578 and pDB579, respectively. Soluble recombinant AtPARN was obtained after the expression in pMAL-p2X or after refolding from the inclusion bodies as described below, obtained from the pMAL-c2X based construct. The latter preparation was free of contamination with nonspecific nucleases and was used for the experiment shown in Figure 2.

Plant constructs

All plant constructs were based on the binary vector pCAMBIA1300 (CAMBIA; Fig. 6). First, a 300-bp-long fragment containing the pea Rubisco small subunit 3′UTR/polyadenylation signal (GB #AF30985) was cloned into SalI/PstI sites, resulting in the construct pDB588. Next, the AtPARN fragment amplified with oDB613 and oDB614, that included 240 bp of the 5′ flanking sequence, was cloned into pDB588 via an intermediate construct, resulting in pDB596. Subsequently, a construct containing a larger fragment (895 bp) of the 5′-flanking region was created, by replacing the BamHI-BsrGI fragment of pDB596 with a oDB673/oDB614 PCR product, resulting in pDB604. To create the AtPARN-GFP fusion constructs, the GFP coding region from mGFP4 was amplified with primers oDB676/oDB677 and cloned in-frame as a C-terminal translational fusion with AtPARN ORF, at NotI and SalI sites. The AtPARN-GFP fusion with 240 bp of upstream sequence was named pDB600. Using a procedure similar to the one described above, BamHI-BsrGI region of pDB600 was replaced by the PCR products obtained using the *Arabidopsis* genomic DNA as a template and primers oDB674/oDB614 and oDB673/oDB614, resulting in the AtPARN-GFP fusion constructs containing 3.2 kb (pDB603) and 895 bp (pDB602) of the 5′-flanking sequence, respectively. For transient expression in onion epidermal cells, the AtPARN cDNA was cloned into the NcoI site of pAVA393 (von Arnim et al. 1998) under the control of the 35S promoter, in frame with the downstream mGFP5 gene (construct pDB614).

Catalytically inactive AtPARN constructs

To introduce the catalytically inactive form of AtPARN into *Arabidopsis*, the BamHI-BsrGI fragment of pDB604 was replaced by the corresponding DNA fragment with two amino acid substitutions, D66A and E68A. Self-complementary oligonucleotides oDB769 and oDB770 containing desired mutations were paired with the downstream (oDB730) and upstream (oDB673) primers, respectively, to amplify the two fragments of PARN gene, which were then fused by overlap extension PCR (Ho et al. 1989). The resulting mutant fragment was cut with BamHI and BsrGI, gel-purified, and ligated into the pDB604 cut with the same enzymes, producing plasmid pDB612. For production of the catalytically inactive AtPARN in *E.coli*, the BamHI-BsrGI fragment of pDB578 was exchanged for the equivalent piece obtained as described above, except that Z2590/oDB730 and oDB769/oDB730 primer combinations were used on the pDB578 plasmid as a template. The resulting construct was named pDB581.

T-DNA collection screening, plant genotyping, and expression and localization assays

T-DNA alleles of AtPARN

T-DNA populations (in WS ecotype) maintained at the University of Wisconsin Biotechnology Center were screened by PCR for T-DNA insertions in *AtPARN* using a T-DNA-specific primer, JL202 (all oligonucleotides used in this work are listed in Table 1) in combination with either gene-specific primer oDB556 or oDB557, according to the instructions provided on the UWBC Web site (www.biotech.wisc.edu/Arabidopsis). PCR products were verified by Southern analysis using the DNA fragment amplified by oDB556 and oDB557 as a probe. The T-DNA/genomic-DNA junctions were further authenticated by sequencing using a T-DNA left border-specific primer, JL270. Three T-DNA insertion

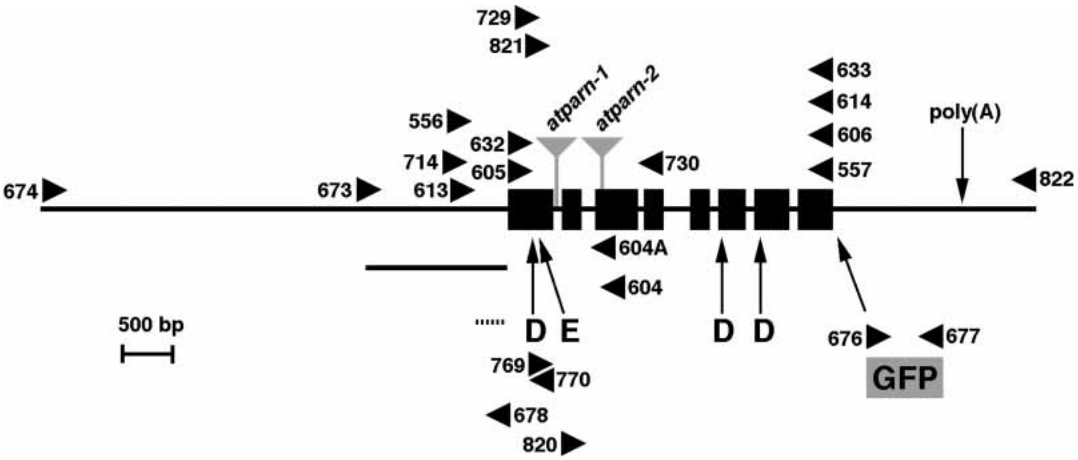

FIGURE 6. AtPARN constructs used in this work and positions of the oligonucleotides. The locations of the oligonucleotide primers mentioned in the Materials and Methods are indicated. Exons are shown as black bars. Approximate positions of the four conserved catalytically important residues, as well as the position of the polyadenylation signal are indicated. The green fluorescent protein (GFP) open reading frame (ORF) was fused onto the last exon of AtPARN for localization studies as shown. Transgene constructs containing either 900 bp or 3000 bp of the 5′ flanking sequence (indicated by solid black lines) were able to complement the *atparn* alleles, but the 240-bp 5′ flanking fragment construct (indicated by the dotted line) was unable to complement the mutant alleles.

TABLE 1. Oligonucleotides used (see Fig. 6 for primer locations)

Name	Sequence
JL202	5′-CATTTTATAATAACGCTGCGGACATCTAC
JL270	5′-TTTCTCCATATTGACCATCATACTCATTG
oDB556	5′-TCACAAAACGGTACCGTTTCCTCGGAATC
oDB557	5′-ACTCGTAGCAGTTTCGACTTCAACTCTAT
oDB604	5′-GCTGGTGGATCAAATGTGAGTTCTTGACGA
oDB604A	5′-TGTGAGTTCTTGACGAGGAA
0DB605	5′-CCGTTCACATATGCGCCGGCACAA
oDB606	5′-ATTACTCGAGGCAGTTTCGACTTCAACTCTATT
oDB613	5′-TTGGATCCTGTTGTTGTTCATCGGGAAAA
oDB614	5′-TCCATCTTCTCTTTTCCATGGCATTACTCGTAGCAGTTTCGACTTCAACTC
oDB632	5′-TCTCGAGATGGGTCATCATCATCATCATCATGAAAATTTGTATTTTCAAGGTATGCGCCGGCACAAGCGA
oDB633	5′-GGAAGCTTAATTACTCGTAGCAGTTTCGACT
oDB635	5′-CAGCTGTTGCCCGTCTCACTGGTGAA
oDB663	5′-GCGTAATACGACTCACTATAGGCTATCTCAGCAGAGAAGTC
oDB664	5′-TGTGAGCAAGCTTCAAGAA
oDB665	5′-CTATCTCAGCAGAGAAGTC
oDB666	5′-GCGTAATACGACTCACTATAGGTGTGAGCAAGCTTCAAGAA
oDB667	5′-AAGCATTCTATCCGTTGGA
oDB668	5′-GCGTAATACGACTCACTATAGGAAGCATTCTATCCGTTGGA
oDB669	5′-GTAGGTTGGAATCGACGTTCTCCGGAACACATATT
oDB670	5′-GTCGATTCCAACCTACGCAAGGAGACAACGAGATC
oDB671	5′-TCAGCCATCAGGGTTCTTC
oDB672	5′-GGGTAATACGACTCACTATAGGTCAGCCATCAGGGTTCTTC
oDB673	5′-GCATTTTGCATGGATCCATGCTCTG
oDB674	5′-GGTTAACACAGCCAATACATATACAACATC
oDB676	5′-ATAATCATGAGTAAAGGAGAAGAAC
oDB677	5′-TATGTCGACTTATTTGTATAGTTCATCCA
oDB678	5′-CATTTTTGAACGGAGAGAGAGA
oDB714	5′-CCGCCATGACGATTCGAGTTCCCAAGC
oDB729	5′-CAGGCGCGCCGTGGCGAGACTCCTTAG
oDB730	5′-GGGCCCATGTACACAAGATCTCCAAAATGCTT
oDB743	5′-TTTCTAGAACATGCACTGATAATATGCTA
oDB744	5′-TTGAGCTCTTCTTGCGTTAGGAGTTCGATGA
oDB745	5′-TTTCTGCAGCAATAGTACAGGTGGCTGATTAC
oDB746	5′-TTCTCGAGTCAACAATGCCTCGAATGCTCCC
oDB769	5′-GTGGCGATTGCCCTTGCGATGACTGGCGTG
oDB770	5′-CACGCCAGTCATCGCAAGGGCAATCGCCAC
oDB777	5′-CTTAACGTAGAGACCTTAGAA
oDB778	5′-GTAGAAGTGATCTCTTGATTG
oDB786	5′-GTACAAAGTCACATCTAAATTTCC
oDB802	5′-ACAAGGTACTCTACAACGTAT
oDB803	5′-GGTACTCTACAACGTATGATG
oDB820	5′-CCACCAGCTCATGAATTTCTCTGTCA
oDB821	5′-ACTCCGCCGAGAAATTCGCC
oDB822	5′-CGTTCTCCACACGATTGCCG
oDB824	5′-ATATAGACCACCGTTACCAAC
oDB825	5′-TGTGTTTCTATATGTTGTCAA
oDB826	5′-GCAAGTGTTGTGTTGTACTTT
oDB827	5′-AAGGAGTTGCATTTTACAGGT
oDB828	5′-AATGAACCTCGAGTACTGTAA
oDB829	5′-ATGTGACTAGTTTTGTTGAGG
oDB833	5′-ATTGACATACTTTACCACAAG
oDB834	5′-GTGTTTTTCATCTGATCTGT
oDB835	5′-TAAGCGAAAACAATGCTGCT
0DB853	5′-UACUCAUCAUACGUUGUAGAGUACCUUGUAidT
oDB938	5′-AAAGGGCAGAGAGCGAACTGGAGAA
oDB950	5′-GGTGCAGGACATACCGTTCCAGAAT
Z2590	5′-CGACGCATATGAAAATCGAAGAAGGTAAACTG
Z2658	5′-ATCGCTGCAGTTGGACGATCGATGATAAG
Z2858	5′-GCGTCTAGAACACACAGGGGCGCTATCGCA

alleles were found in the BASTA population: 557B14 (*atparn-3*), 556B14 (*atparn-1*), and 557B40 (*atparn-2*), located 364 bp, 408 bp, and 728 bp downstream of the ATG codon, respectively. Actual sequences of the T-DNA/genomic-DNA junctions are as follows (T-DNA left border sequences are italicized, short scrambled sequences between the T-DNA and genomic DNA are shown in lowercase):

557B14 (*atparn-3*)—364 bp downstream of ATG codon: *TTTC CCGGACATGAAGCCATTTACA*-tgaagccatcg-TACCCGTTAG TTTCTCTTTCTCTTTTCTTTTAAATACCCGTTA;
556B14 (*atparn-1*)—408 bp downstream of ATG codon: *TTTCCCG GACATGAAGCCATTTACAATTGAATATATCCTG*-ttagttaa-ACAC AATTGAAGCTAAAGAGAAAGAGAAAGA;
557B40 (*atparn-2*)—728 bp downstream of ATG codon: *TTTCC CGGACATGAAGCCATTTACAATTGAATATATCC*-TGAAAA TGCTACACGGCGAGGACGGAATTGATTCATCGGGTG.

T-DNA allele of At3g25430

The null allele of At3g25430 (line SALK_078011) was generated by Joseph Ecker′s group at the Salk Institute (Salk Institute Genome Analysis Laboratory) as a part of the published collection of T-DNA insertion lines (Alonso et al. 2003), and obtained via the Arabidopsis Biological Resource Center at Ohio State University. The T-DNA in SALK_078011 is inserted in exon 1 of At3g25430. Screening of this line′s progeny was conducted using PCR primer pairs oDB950 (sense) and oDB938 (antisense), which produce the 744-bp-long product from the wild-type allele only, and oDB635 (T-DNA-specific primer) and oDB938. The latter pair produce a 400-bp product from the mutant allele only. Numerous homozygous mutant plants were identified, and none had any obvious phenotype.

Expression survey of AtPARN

RNA was prepared using an adaptation of the guanidinium thiocyanate/acid phenol extraction method (Chomczynski and Sacchi 1987). *Arabidopsis* tissue (50–100 mg) was harvested into 1.5-mL Eppendorf tubes, and homogenized in 400 μL of homogenization buffer (4 M guanidinium thiocyanate, 25 mM sodium citrate pH 7.0, 1.5% sodium sarcosyl, 1% β-mercaptoethanol) with a plastic pestle. Extract was supplemented with 40 μL of 3 M sodium acetate (pH 5.2) and 500 μL of phenol-chloroform mix, vortexed, incubated on ice for 10 min and centrifuged. The supernatant was removed, and nucleic acids precipitated by adding an equal volume of isopropanol. The RNA pellet was redissolved in 150 μL of homogenization buffer, reprecipitated with isopropanol, and reprecipitated again with lithium chloride. After the DNAse digestion and extraction with phenol-chloroform, RNA was precipitated with sodium acetate/ethanol. The final pellet was washed with 70% ethanol, dried, redissolved in 27 μL RNAse-free water, and stored at −80°C. The cDNA synthesis was performed using Superscript II (Invitrogen) on 10 μL of the above total RNA preparation with 0.5 μg dT_{17} primer in a standard 20 μL reaction. After 1 h at 37°C, the reaction was heated at 75°C for 15 min, diluted to 100 μL with TE, and stored at −80°C. For the 50-μL PCR reaction, 1 μL of this preparation was used as template with AtPARN gene-specific primers oDB605 and oDB606.

Biolistic assays

Onion epidermal peels were prepared for transformation as described (Varagona et al. 1992). The protocol for DNA preparation and biolistic delivery was essentially as described by Sanford et al. (1993). Briefly, 30 mg of 1.6 μM gold particles were suspended in 120 μL of sterile 50% ethanol and kept suspended by constant vortexing. Then, 25 μL of solution (enough for 3 bombardments/construct) was added to a microfuge tube containing 2.5 μL of DNA (1 μg/μL) of the appropriate plasmid construct. To this tube was added 25 μL of 2.5 M $CaCl_2$ and then 10 μL of 1 M spermidine (free base) with continued vortexing for about 3 min. The DNA-coated particles were spun down for 15 sec, washed with 70% ethanol, and resuspended in anhydrous 100% ethanol.

For transformation, the gold particles were propelled using a "flying-disc" helium-driven biolistic device that uses a fast-opening valve to generate the pressure shock wave. A total of 8 μL of DNA-coated particles were spread on each disc and placed under a gentle stream of air which rapidly evaporated the 100% ethanol, leaving evenly distributed particles. These discs were then mounted into holders and used to transform onion epidermal peels.

Genotyping assays for the complementation of the null allele of AtPARN

PCR on leaf clips (Klimyuk et al. 1993) was used for plant genotyping, as well as for the verification of transformants. The presence of AtPARN gene T-DNA knockouts was established by means of PCR analysis employing combination of left border primers JL202 or JL270 with one of the downstream (oDB604 or oDB730) or upstream (oDB556 or oDB729) primers. Amplification with primer pairs oDB604/oDB556 or oDB729/oDB730 was used to establish the presence of the wild-type AtPARN allele in the segregating progeny of the heterozygous knockout plants. Multiplex PCR for simultaneous detection of the AtPARN T-DNA insertions and the wild-type AtPARN was carried out using primer combinations oDB729/oDB730/JL270 or oDB729/oDB730/JL202.

Following the selection of the transformants on hygromycin plates, the presence of the AtPARN transgenes was confirmed by PCR with primers M13/oDB678 for the wild-type AtPARN transgene constructs, or with primers oDB676/oDB677 for the PARN-GFP fusions. Complementation of the null allele by all of the introduced AtPARN transgenes except the construct pDB596 (below) was then assayed using multiplex PCR with primers oDB820/oDB821/oDB822. In this case, the PARN fragment introduced on a transgene cannot be amplified, because the primer oDB822 lies outside of the region included in the construct. Amplification from the endogenous *AtPARN* gene produced two bands, that is, products of the oDB821/oDB822 and oDB820/oDB822 primer pairs, with a size difference of 200 bp. The absence of the larger of the two products due to the inserted T-DNA would be indicative of the complementation.

For genotyping of the plants transformed with the construct pDB596, the primer pair oDB714/oDB604A was used, which amplify the fragment from the endogenous wild-type, but not from the introduced AtPARN transgene, across the position of the T-DNA insertion. Absence of such a band would mean the absence of noninterrupted wild-type PARN gene. The band was present in all plants studied. The numbers of plants that were tested for the

complementation with the different AtPARN constructs and the numbers of complemented positives found are listed in Table 2.

Microscopy

For observation of embryos (Fig. 3), developing seeds were fixed in HistoChoice (Amresco), cleared using modified Hoyer's solution (7.5 g gum arabic, 100 g chloral hydrate, 5 mL glycerol, and 30 mL water), mounted, and viewed on an Olympus BX60 using Nomarski optics. GFP fluorescence (Figs. 2, 3) was viewed using the 41001 filter cube. Protoplasting of the leaves from transgenic plants to facilitate the visualization of GFP was conducted as described by Abel and Theologis (1994).

AtPARN enzymatic assays

Soluble AtPARN, expressed in *E.coli* as MBP fusion in pDB579 (based on pMAL-p2X), exhibited specific poly(A) degrading activity. However, such preparations were often contaminated with copurifying nonspecific nuclease activity. Therefore, the recombinant protein was refolded from the inclusion bodies as described below, which resulted in the active enzyme preparation essentially free from nonspecific nucleases. For the AtPARN assays, a 102-bp DNA fragment containing T7 promoter and 20 nucleotide poly(A) or poly(T) tail (Chekanova et al. 2000) was used as a template to generate radiolabeled RNA substrates. RNA was synthesized with an Ampliscribe T7 kit (Epicentre) in the presence of [^{32}P]-UTP (3000Ci/mMol, Amersham). Resulting RNAs were treated with DNAse, extracted with phenol/chloroform, and precipitated. Purified RNA substrates were incubated with protein samples under conditions similar to those described for human PARN (Ren et al. 2002), except that the reaction buffer used did not contain polyvinyl alcohol. Aliquots of 30 μL (1–3×10^{4}cpm and 1–5 μg of recombinant MBP-AtPARN per time point) were taken at specified time intervals and immediately mixed with 60 μL of 2× protease buffer (200 mM Tris-HCl pH7.9, 300 mM NaCl, 25 mM EDTA, 2%SDS) and 30 μL of Proteinase K solution (800 μg/mL Proteinase K, 200 μg/mL Glycogen, 80 μg/mL total yeast RNA), incubated at 37°C for 1 h, and precipitated with NaOAc/EtOH overnight. Resulting RNA samples were separated on 8% PAAG containing 7 M urea, and exposed to a PhosphorImager screen (Molecular Dynamics).

Expression and purification of AtPARN

Manufacturer (New England Biolabs) recommended procedures were employed for expression and purification of the MBP-AtPARN fusions. Generally, 0.5 L of rich media, or LB supplemented with 0.2% glucose and 0.1–0.15 mg/mL ampicillin was inoculated with 1/100 volume of overnight culture of appropriate construct in BL21 or Origami B (Novagen) host. Cultures were grown at 37°C to OD_{600} of 0.6–0.8, cooled, and induced with 0.3 mM IPTG overnight at room temperature. After harvesting, the cell pellet was resuspended in 20 mL of column buffer (20 mM Tris-HCl pH 7.5, 200 mM NaCl, 10% glycerol, 0.2% Triton X-100, 1 mM EDTA, 1 mM PMSF, 1 mM DTT) and subjected to three freeze-thaw cycles. Cells were lysed by sonication, and the soluble fraction was separated by centrifugation at 40,000*g* for 45 min. The pellet was resuspended in fresh 20 mL of column buffer and stored at −80°C. Two mL of this suspension was mixed with 14 mL of 7M urea and left rocking overnight at 4°C. The solution was clarified by centrifugation (40,000*g*, 30 min), and diluted 1.5-fold by addition of 8 mL of AtPARN storage buffer SB (20 mM HEPES pH 8.2, 100 mM KCl, 1.5 mM $MgCl_2$, 0.2 mM EDTA, 0.5 mM DTT). After another 6 h of rocking at 4°C, solution was again clarified, and two more twofold SB dilution cycles were performed with mixing at 4°C for 6 h to overnight. The final clarified dilution containing ~1.15 M urea was concentrated 10-fold on a Vivaspin 10-kDa ultraconcentrator (Vivascience), and dialyzed against two 2-L changes of SB supplemented with 1 mM oxidized/0.2 mM reduced glutathione. No visible precipitate formed at this stage. Dialyzed protein was concentrated to a final volume of 0.5 mL and stored at −80°C.

An aliquot of 250 μL of refolded AtPARN was diluted with 5 mL of column buffer and mixed overnight with 1 mL of washed amylose resin at 4°C. The column was drained, washed with column buffer supplemented with 1 M KCl, and then with SB and eluted with 10 × 0.5 mL aliquots of 10 mM maltose in SB. Fractions containing MBP-AtPARN were pooled and concentrated.

TABLE 2. Results of the complementation tests with the various AtPARN constructs

Construct	5′-upstream region, bp	# Plants tested	# Complemented
pDB596	240	63	0
pDB603	3220	15	1
pDB602	895	81	12
pDB600	240	26	0
pDB604	895	26	13
pDB612	895	101	0

S. pombe constructs and techniques

To prepare the *S. pombe* PARN gene disruption cassette, the following three PCR-generated DNA fragments were amplified and joined: (1) the 994-bp fragment from the *S. pombe* PARN gene 5′ flanking region, generated with primers oDB744 and oDB743 with genomic *S. pombe* DNA as template; (2) the *S. cerevisiae LEU2* gene (which complements the *S. pombe leu1* mutation), generated with primers Z2658 and Z2858 using Ycp111 (Gietz and Sugino 1988) as template; and (3) the 1084-bp fragment from the *S. pombe* PARN gene 3′ flanking region, generated with primers oDB745 and oDB746 with genomic *S. pombe* DNA as template. The resulting fragments were digested with SacI + XbaI, XbaI + PstI, and PstI + XhoI, respectively, joined via three-way ligation and cloned into Bluescript SK(+). The resulting disruption cassette was excised with SacI + XhoI, and integrated into the diploid *S. pombe* strain produced by mating of FY527 (*h*$^-$ *his3-D1 ura4-D18 leu1−32 ade6-M216*) and FY528 (*h*$^+$ *his3-D1 ura4-D18 leu1−32 ade6-M216*; Liang and Forsburg 2001). Integrants were verified by PCR analysis and Southern blotting, sporulated, and patched onto Leu$^+$ and Leu$^-$ media to isolate *parn*$^+$ and *parn* mutant progeny. The general *S.pombe* techniques and media were according to Moreno et al. (1991).

C. elegans techniques

Double-stranded RNA targeting the two *C. elegans* PARN homologs, K10C8.1 and Y57A10A.25, were produced as follows. For

microinjection, the 740-nt-long K10C8.1 dsRNA was produced by annealing of the T7 transcripts made from the templates that were amplified by PCR using oDB663 and oDB664 (top strand, T7 polymerase promoter included in oDB663) and oDB665 and oDB666 (bottom strand, T7 polymerase promoter included in oDB666). This dsRNA targeted exon 3 (the longest exon) of K10C8.1. For Y57A10A.25, templates were produced by overlap extension PCR (Ho et al. 1989) -mediated fusion of two PCR fragments, 480 bp and 536 bp, corresponding to the exons 2 and 3 of Y57A10A.25. Exon 2 fragment was amplified with oDB667 and oDB669, and exon 3 with oDB670 and oDB670. Overlap introduced into the 5′ halves of the primers oDB669 and oDB670 was used to anneal the products, and the fused 1016-bp product was amplified by the external primers oDB667 and oDB671. The T7 promoter for transcribing either top or bottom strands of the resulting fusion fragment was then introduced through reamplification with oDB668 (which contains the T7 promoter sequence, for top strand) and oDB671, or with oDB667 and oDB672 (T7 promoter for transcribing the bottom strand). The in vitro transcripts were quantitated and annealed, and the extent of annealing was verified by agarose gel electrophoresis prior to microinjection. *C. elegans* culture and dsRNA microinjection to induce RNAi were done as described by Grishok et al. (2000).

For RNAi by feeding, the PCR-derived templates were first cloned into the dual T7 promoter vector L4440, as follows. First, the Y57A10A.25 exon 2/3 PCR chimera was cleaved at the internal SacI sites, which resulted in removal of ~60 bp from the 5′ end and ~110 bp from the 3′ end, and cloned into the SacI site of L4440. Into the resulting plasmid, the K10C8.1 exon 3 fragment was then cloned as NcoI/blunt fragment after cleaving off some 120 bp from its 3′ end using an internal NcoI site. RNAi by feeding was induced according to the protocol described by Timmons et al. (2001). Neither the feeding random-sequence RNA nor the dual RNAi against the two *C. elegans* PARN homologs has any effect on brood size, embryo hatching, or adult worms. As a control, *POS-1* RNAi knockdown performed in parallel resulted in near 100% embryonic lethality

RNA techniques and LM-PAT

Polyadenylated and polyuridilated RNA substrates for AtPARN assays were synthesized from templates and according to procedures described by Chekanova et al. (2000). Capped RNA was produced according to Stripecke and Hentze (1992). Total RNA isolation from *S. pombe* and measurements of the poly(A) tails lengths were carried out as described by Chekanova et al. (2001) and Sachs and Davis (1989).

LM PAT assay for poly(A) tail length was adapted from the siRNA 3′ end identification procedure described by Xie et al. (2003). Briefly, 50–100 seeds containing embryos from torpedo to bent cotyledon stages of development were collected, and total RNA was purified using an Arcturus PicoPure kit according to the instructions provided by the manufacturer (including the DNAse treatment step). Total RNA was 3′ end-tagged with the 5′ phosphorylated RNA adaptor oligonucleotide oDB853 and RNA ligase, and reverse transcribed using SuperScript II enzyme (Life Technologies) and the oDB802 primer that is complementary to the adaptor oligonucleotide. Diluted cDNA was used as a template for PCR with oDB802 as antisense primer and oDB777 (for PRL1), oDB828 (for cruciferin), oDB825 (for oleosin), or oDB835 (for LEC1-like) as sense primer, using a touchdown profile (initial annealing at 59°C, then decreasing by 1°C per cycle until 48°C was reached, and the 33 additional cycles at 48°C annealing). Diluted first-round products were subjected to the nested PCR under the same conditions, using oDB803 as antisense primer and oDB778 (for PRL1), oDB829 (for cruciferin), oDB826 (for oleosin), or oDB834 (for LEC1-like) as sense primer. Products were authenticated by Southern hybridization with the following gene-specific oligonucleotides as probes: for PRL1, oDB786; for cruciferin, oDB827; for oleosin, oDB824; and for LEC1-like, oDB833. RNaseH treatments prior to LM PAT were carried out as described previously (Chekanova et al. 2001).

ACKNOWLEDGMENTS

We thank Dr. Alla Grishok for the help with RNAi in *C. elegans*. We thank Drs. K. Rathore, L. Kunst, J. Harada, and S. Naito for the GUS reporter lines, and Dr. S. Forsburg for *S. pombe* materials. Some of the *Arabidopsis* genetic stocks used in this paper were obtained through the Arabidopsis Biological Resource Center. We also thank USDA (award #2003-35304-13210 to D.A.B.), NSF (award #9874580 to D.A.B.), SUNY Basic Biosciences Minigrant program, Dr. Henry Tedeschi, Offices of the Vice President for Research and of the Dean of the College of Arts and Sciences of SUNY–Albany for their support, and Dr. Patty Springer for advice and communicating unpublished data.

The publication costs of this article were defrayed in part by payment of page charges. This article must therefore be hereby marked "advertisement" in accordance with 18 USC section 1734 solely to indicate this fact.

Received April 5, 2004; accepted May 5, 2004.

REFERENCES

Abel, S. and Theologis, A. 1994. Transient transformation of *Arabidopsis* leaf protoplasts: A versatile experimental system to study gene expression. *Plant J.* **5:** 421–427.

Alonso, J.M., Stepanova, A.N., Leisse, T.J., Kim, C.J., Chen, H., Shinn, P., Stevenson, D.K., Zimmerman, J., Barajas, P., Cheuk, R., et al. 2003. Genome-wide insertional mutagenesis of *Arabidopsis thaliana*. *Science* **301:** 653–657.

Apuya, N.R., Yadegari, R., Fischer, R.L., Harada, J.J., Zimmerman, J.L., and Goldberg, R.B. 2001. The *Arabidopsis* embryo mutant schlepperless has a defect in the chaperonin-60 α gene. *Plant Physiol.* **126:** 717–730.

Beese, L.S. and Steitz, T.A. 1991. Structural basis for the 3′–5′ exonuclease activity of *Escherichia coli* DNA polymerase I: A two metal ion mechanism. *EMBO J.* **10:** 25–33.

Boutet, S., Vazquez, F., Liu, J., Beclin, C., Fagard, M., Gratias, A., Morel, J.B., Crete, P., Chen, X., and Vaucheret, H. 2003. Arabidopsis HEN1: A genetic link between endogenous miRNA controlling development and siRNA controlling transgene silencing and virus resistance. *Curr. Biol.* **13:** 843–848.

Bowman, J.L. and Koornneef, M. 1994. Embryogenesis. In *Arabidopsis. An atlas of morphology and development* (ed. J.L. Bowman), pp. 351–401. Springer-Verlag, New York.

Butler, J. 2002. The yin and yang of the exosome. *Trends Cell Biol.* **12:** 90–96.

Cao, D. and Parker, R. 2001. Computational modeling of eukaryotic mRNA turnover. *RNA* **7:** 1192–1212.

Chan, M.T. and Yu, S.M. 1998. The 3′ untranslated region of a rice α-amylase gene functions as a sugar-dependent mRNA stability

determinant. *Proc. Natl. Acad. Sci.* **95:** 6543–6547.
Chekanova, J.A., Shaw, R.J., Wills, M.A., and Belostotsky, D.A. 2000. Poly(A) tail-dependent exonuclease AtRrp41p from *Arabidopsis thaliana* rescues 5.8 S rRNA processing and mRNA decay defects of the yeast ski6 mutant and is found in an exosome-sized complex in plant and yeast cells. *J. Biol. Chem.* **275:** 33158–33166.
Chekanova, J.A., Shaw, R.J., and Belostotsky, D.A. 2001. Analysis of an essential requirement for the poly(A) binding protein function using cross-species complementation. *Curr. Biol.* **11:** 1207–1214.
Chekanova, J., Dutko, J.A., Mian, I.S., and Belostotsky, D.A. 2002. *Arabidopsis thaliana* exosome subunit AtRrp4p is a hydrolytic 3′–5′ exonuclease containing S1 and KH RNA-binding domains. *Nucleic Acids Res.* **30:** 695–700.
Chen, C.Y. and Shyu, A.B. 2003. Rapid deadenylation triggered by a nonsense codon precedes decay of the RNA body in a mammalian cytoplasmic nonsense-mediated decay pathway. *Mol. Cell Biol.* **23:** 4805–4813.
Chen, C.-Y.A., Xu, N., and Shyu, A.-B. 1995. mRNA decay mediated by two distinct AU-rich elements from c-fos and granulocyte-macrophage colony-stimulating factor transcripts: Different deadenylation kinetics and uncoupling from translation. *Mol. Cell. Biol.* **15:** 5777–5788.
Chen, X., Liu, J., Cheng, Y., and Jia, D. 2002. HEN1 functions pleiotropically in *Arabidopsis* development and acts in C function in the flower. *Development* **129:** 1085–1094.
Chiba, Y., Ishikawa, M., Kijima, F., Tyson, R.H., Kim, J., Yamamoto, A., Nambara, E., Leustek, T., Wallsgrove, R.M., and Naito, S. 1999. Evidence for autoregulation of cystathionine γ-synthase mRNA stability in *Arabidopsis*. Science **286:** 1371–1374.
Chiba, Y., Sakurai, R., Yoshino, M., Ominato, K., Ishikawa, M., Onouchi, H., and Naito, S. 2003. S-adenosyl-L-methionine is an effector in the posttranscriptional autoregulation of the cystathionine γ-synthase gene in *Arabidopsis*. *Proc. Natl. Acad. Sci.* **100:** 10225–10230.
Chiba, Y., Johnson, M.A., Lidder, P., Vogel, J.T., van Erp, H., and Green, P.J. 2004. AtPARN is an essential poly(A) ribonuclease in *Arabidopsis*. *Gene* **328:** 95–102.
Chomczynski, P. and Sacchi, N. 1987. Single-step method of RNA isolation by acid guanidinium thiocyanate-phenol-chloroform extraction. *Anal. Biochem.* **162:** 156–159.
Clough, S.J. and Bent, A.F. 1998. Floral dip: A simplified method for Agrobacterium-mediated transformation of *Arabidopsis thaliana*. *Plant J.* **16:** 735–743.
Copeland, P.R. and Wormington, M. 2001. The mechanism and regulation of deadenylation: Identification and characterization of *Xenopus* PARN. *RNA* **7:** 875–886.
Dehlin, E., Wormington, M., Korner, C.G., and Wahle, E. 2000. Cap-dependent deadenylation of mRNA. *EMBO J.* **19:** 1079–1086.
Dupressoir, A., Morel, A.P., Barbot, W., Loireau, M.P., Corbo, L., and Heidmann, T. 2001. Identification of four families of yCCR4– and Mg2+-dependent endonuclease-related proteins in higher eukaryotes, and characterization of orthologs of yCCR4 with a conserved leucine-rich repeat essential for hCAF1/hPOP2 binding. *BMC Genomics* **2:** 9.
Frischmeyer, P.A., van Hoof, A., O'Donnell, K., Guerrerio, A.L., Parker, R., and Dietz, H.C. 2002. An mRNA surveillance mechanism that eliminates transcripts lacking termination codons. *Science* **295:** 2258–2261.
Gao, M., Fritz, D.T., Ford, L.P., and Wilusz, J. 2000. Interaction between a poly(A)-specific ribonuclease and the 5′ cap influences mRNA deadenylation rates in vitro. *Mol. Cell* **5:** 479–488.
Gietz, R.D. and Sugino, A. 1988. New yeast-*Escherichia coli* shuttle vectors constructed with in vitro mutagenized yeast genes lacking six-base pair restriction sites. *Gene* **74:** 527–534.
Gil, P. and Green, P.J. 1996. Multiple regions of the *Arabidopsis* SAUR-AC1 gene control transcript abundance: The 3′ untranslated region functions as an mRNA instability determinant. *EMBO J.* **15:** 1678–1686.
Gil, P., Liu, Y., Orbovic, V., Verkamp, E., Poff, K.L., and Green, P.J. 1994. Characterization of the auxin-inducible SAUR-AC1 gene for use as a molecular genetic tool in *Arabidopsis*. *Plant Physiol.* **104:** 777–784.
Grishok, A., Tabara, H., and Mello, C.C. 2000. Genetic requirements for inheritance of RNAi in *C. elegans*. *Science* **287:** 2431–2432.
Higgs, D.C. and Colbert, J.T. 1994. Oat phytochromeA mRNA degradation appears to occur via two distinct pathways. *Plant Cell* **6:** 1007–1019.
Hirai, M.Y., Fujiwara, T., Goto, K., Komeda, Y., Chino, M., and Naito, S. 1994. Differential regulation of soybean seed storage protein gene promoter-GUS fusions by exogenous applied methionine in transgenic *Arabidopsis thaliana*. *Plant Cell Physiol.* **35:** 927–934.
Ho, S.N., Hund, H.D., Horton, R.M., Pullen, J.K., and Pease, L.R. 1989. Site-directed mutagenesis by overlap extension using the polymerase chain reaction. *Gene* **77:** 51–59.
Isshiki, M., Yamamoto, Y., Satoh, H., and Shimamoto, K. 2001. Nonsense-mediated decay of mutant waxy mRNA in rice. Plant Physiol. **125:** 1388–1398.
Johnson, M.A., Perez-Amador, M.A., Lidder, P., and Green, P.J. 2000. Mutants of *Arabidopsis* defective in a sequence-specific mRNA degradation pathway. *Proc. Natl. Acad. Sci.* **97:** 13991–13996.
Kamath, R.S., Fraser, A.G., Dong, Y., Poulin, G., Durbin, R., Gotta, M., Kanapin, A., Le Bot, N., Moreno, S., Sohrmann, M., et al. 2003. Systematic functional analysis of the *Caenorhabditis elegans* genome using RNAi. *Nature* **421:** 231–237.
Kastenmayer, J.P. and Green, P.J. 2000. Novel features of the XRN-family in *Arabidopsis*: Evidence that AtXRN4, one of several orthologs of nuclear Xrn2p/Rat1p, functions in the cytoplasm. *Proc. Natl. Acad. Sci.* **97:** 13985–13990.
Kidner, C.A. and Martienssen, R.A. 2004. Spatially restricted microRNA directs leaf polarity through ARGONAUTE1. *Nature* **428:** 81–84.
Klimyuk, V.I., Carroll, B.J., Thomas, C.M., and Jones, J.D. 1993. Alkali treatment for rapid preparation of plant material for reliable PCR analysis. *Plant J.* **3:** 493–494.
Koornneef, M., Hanhart, C.J., Hilhorst, H.W.M., and Karssen, C.M. 1989. In vivo inhibition of seed development and reserve protein accumulation in recombinants of *abscisic acid* biosynthesis and responsiveness mutants in *Arabidopsis thaliana*. *Plant Physiol.* **90:** 463–469.
Korner, C.G., Wormington, M., Muckenthaler, M., Schneider, S., Dehlin, E., and Wahle, E. 1998. The deadenylating nuclease (DAN) is involved in poly(A) tail removal during the meiotic maturation of *Xenopus* oocytes. *EMBO J.* **17:** 5427–5437.
Kreft, O., Hoefgen, R., and Hesse, H. 2003. Functional analysis of cystathionine γ-synthase in genetically engineered potato plants. *Plant Physiol.* **131:** 1843–1854.
Lai, W.S., Kennington, E.A., and Blackshear, P.J. 2003. Tristetraprolin and its family members can promote the cell-free deadenylation of AU-rich element-containing mRNAs by poly(A) ribonuclease. *Mol. Cell Biol.* **23:** 3798–3812.
Lejeune, F., Li, X., and Maquat, L.E. 2003. Nonsense-mediated mRNA decay in mammalian cells involves decapping, deadenylating, and exonucleolytic activities. *Mol. Cell* **12:** 675–687.
Liang, D.T. and Forsburg, S.L. 2001. Characterization of *Schizosaccharomyces pombe* mcm7(+) and cdc23(+) (MCM10) and interactions with replication checkpoints. *Genetics* **159:** 471–486.
Llave, C., Xie, Z., Kasschau, K.D., and Carrington, J.C. 2002. Cleavage of Scarecrow-like mRNA targets directed by a class of *Arabidopsis* miRNA. *Science* **297:** 2053–2056.
Lue, M.-Y. and Lee, H.-T. 1994. Poly(A) tail shortening of α-amylase mRNAs in vegetative tissues of *Oryza sativa*. *Biochem. Biophys. Res. Comm.* **202:** 1031–1037.
Martinez, J., Ren, Y.G., Nilsson, P., Ehrenberg, M., and Virtanen, A. 2001. The mRNA cap structure stimulates rate of poly(A) removal and amplifies processivity of degradation. *J. Biol. Chem.* **276:** 27923–27929.
Meinke, D.W. 1994. Seed development in *Arabidopsis thaliana*, in *Arabidopsis* (eds. E.M. Meyerowitz and C.R. Somerville), pp. 253–

295. Cold Spring Harbor Laboratory Press, Cold Spring Harbor, NY.

Mitchell, P. and Tollervey, D. 2000. Musing on the structural organization of the exosome complex. *Nat. Struct. Biol.* **7:** 843–846.

———2003. An NMD pathway in yeast involving accelerated deadenylation and exosome-mediated 3′–5′ degradation. *Mol. Cell* **11:** 1405–1413.

Moreno, S., Klar, A., and Nurse, P. 1991. Molecular genetic analysis of fission yeast *Schizosaccharomyces pombe*. *Methods Enzymol.* **194:** 795–823.

Ohme-Takagi, M., Taylor, C.B., Newman, T.C., and Green, P.J. 1993. The effect of sequences with high AU content on mRNA stability in tobacco. *Proc. Natl. Acad. Sci.* **90:** 11811–11815.

Palatnik, J.F., Allen, E., Wu, X., Schommer, C., Schwab, R., Carrington, J.C., and Weigel, D. 2003. Control of leaf morphogenesis by microRNAs. *Nature* **425:** 257–263.

Papp, B., Pal, C., and Hurst, L.D. 2003. Dosage sensitivity and the evolution of gene families in yeast. *Nature* **424:** 194–197.

Petracek, M.E., Dickey, L.F., Huber, S.C., and Thompson, W.F. 1997. Light-regulated changes in abundance and polyribosome association of ferredoxin mRNA are dependent on photosynthesis. *Plant Cell* **9:** 2291–2300.

Ren, Y.G., Martinez, J., and Virtanen, A. 2002. Identification of the active site of poly(A)-specific ribonuclease by site-directed mutagenesis and Fe(2+)-mediated cleavage. *J. Biol. Chem.* **277:** 5982–5987.

Rossak, M., Smith, M., and Kunst, L. 2001. Expression of the FAE1 gene and FAE1 promoter activity in developing seeds of *Arabidopsis thaliana*. *Plant Mol. Biol.* **46:** 717–725.

Sachs, A.B. and Davis. R.W. 1989. The poly(A) binding protein is required for poly(A) shortening and 60S ribosomal subunit-dependent translational initiation. *Cell* **58:** 857–867.

Salles, F.J., Richards, W.G., and Strickland, S. 1999. Assaying the polyadenylation state of mRNAs. *Methods* **17:** 38–45.

Sanford, J.C., Smith, F.D., and Russell, J.A. 1993. Optimizing the biolistic process for different biological applications. *Meth. Enzymol.* **217:** 483–509.

Sheu, J.J., Yu, T.S., Tong, W.F., and Yu, S.M. 1996. Carbohydrate starvation stimulates differential expression of rice α-amylase genes that is modulated through complicated transcriptional and posttranscriptional processes. *J. Biol. Chem.* **271:** 26998–27004.

Sorensen, M.B., Chaudhury, A.M., Robert, H., Bancharel, E., and Berger, F. 2001. Polycomb group genes control pattern formation in plant seed. *Curr. Biol.* **11:** 277–281.

Springer, P.S., McCombie, W.R., Sundaresan, V., and Martienssen, R.A. 1995. Gene trap tagging of *PROLIFERA*, an essential *MCM2-3-5*-like gene in *Arabidopsis. Science* **268:** 877–880.

Springer, P.S., Holding, D.R., Groover, A., Yordan, C., and Martienssen, R.A. 2000. The essential Mcm7 protein PROLIFERA is localized to the nucleus of dividing cells during the G(1) phase and is required maternally for early *Arabidopsis* development. *Development* **127:** 1815–1822.

Stripecke, R. and Hentze, M.W. 1992. Bacteriophage and spliceosomal proteins function as position-dependent cis/trans repressors of mRNA translation in vitro. *Nucleic Acids Res.* **20:** 5555–5564.

Sunilkumar, G., Connell, J.P., Smith, C.W., Reddy, A.S., and Rathore, K.S. 2002. Cotton α-globulin promoter: Isolation and functional characterization in transgenic cotton, *Arabidopsis*, and tobacco. *Transgenic Res.* **11:** 347–359.

Tanzer, M.M. and Meagher, R.B. 1995. Degradation of the soybean ribulose-1,5-bisphosphate carboxylase small-subunit mRNA, SRS4, initiates with endonucleolytic cleavage. *Mol. Cell. Biol.* **15:** 6641–6652.

Timmons, L., Court, D.L., and Fire, A. 2001. Ingestion of bacterially expressed dsRNAs can produce specific and potent genetic interference in *Caenorhabditis elegans*. *Gene* **263:** 103–112.

Tucker, M. and Parker, R. 2000. Mechanisms and control of mRNA decapping in *Saccharomyces cerevisiae*. *Annu. Rev. Biochem.* **69:** 571–595.

Tucker, M., Valencia-Sanchez, M.A., Staples, R.R., Chen, J., Denis, C.L., and Parker, R. 2001. The transcription factor associated Ccr4 and Caf1 proteins are components of the major cytoplasmic mRNA deadenylase in *Saccharomyces cerevisiae*. *Cell* **104:** 377–386.

Tye, B.K. and Sawyer, S. 2000. The hexameric eukaryotic MCM helicase: Building symmetry from nonidentical parts. *J. Biol. Chem.* **275:** 34833–34836.

Uchida, N., Hoshino, S.I., and Katada, T. 2004. Identification of a human cytoplasmic poly(A) nuclease complex stimulated by poly(A)-binding protein. *J. Biol. Chem.* **279:** 1383–1391.

van Hoof, A. and Green, P.J. 1996. Premature nonsense codons decrease the stability of phytohemagglutinin mRNA in a position-dependent manner. *Plant J.* **10:** 415–424.

van Hoof, A., Frischmeyer, P.A., Dietz, H.C., and Parker, R. 2002. Exosome-mediated recognition and degradation of mRNAs lacking a termination codon. *Science* **295:** 2262–2264.

Varagona, M.J., Schmidt, R.J., and Raikhel, N.V. 1992. Nuclear localization signal(s) required for nuclear targeting of the maize regulatory protein Opaque-2. *Plant Cell* **4:** 1213–1227.

Vasudevan, S. and Peltz, S.W. 2001. Regulated ARE-mediated mRNA decay in *Saccharomyces cerevisiae*. *Mol. Cell* **7:** 1191–1200.

von Arnim, A.G., Deng, X.W., and Stacey, M.G. 1998. Cloning vectors for the expression of green fluorescent protein fusion proteins in transgenic plants. *Gene* **221:** 35–43.

Wang, H., Wu, H.-m., and Cheung, A.Y. 1996. Pollination induces mRNA poly(A) tail shortening and cell deterioration in flower transmitting tissue. *Plant J.* **9:** 715–727.

Wilusz, C.J., Wormington, M., and Peltz, S.W. 2001. The cap-to-tail guide to mRNA turnover. *Nat. Rev Mol. Cell Biol.* **2:** 237–246.

Winzen, R., Kracht, M., Ritter, B., Wilhelm,A., Chen, C.Y., Shyu, A.B., Muller, M., Gaestel, M., Resch, K., and Holtmann, H. 1999. The p38 MAP kinase pathway signals for cytokine-induced mRNA stabilization via MAP kinase-activated protein kinase 2 and an AU-rich region-targeted mechanism. *EMBO J.* **18:** 4969–4980.

Xie, Z., Kasschau, K.D., and Carrington, J.C. 2003. Negative feedback regulation of dicer-like1 in *Arabidopsis* by microRNA-guided mRNA degradation. *Curr. Biol.* **13:** 784–789.